LBL-13379
Preprint

Lawrence Berkeley Laboratory
UNIVERSITY OF CALIFORNIA

Submitted to Physical Review Letters

NOV 1981
LIBRARY
DOCUMENTS SECTION

DO NUCLEI FLOW AT HIGH ENERGIES?

M. Gyulassy, K.A. Frankel, and H. Stöcker

September 1981

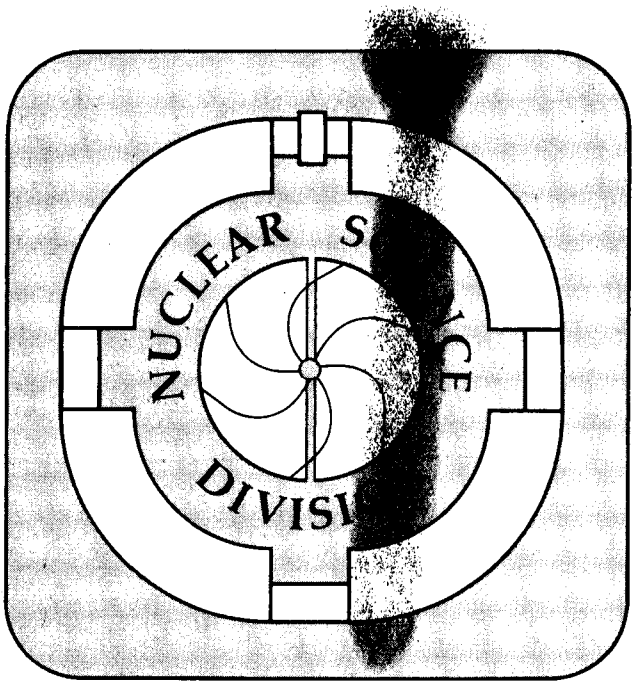

Prepared for the U.S. Department of Energy under Contract W-7405-ENG-48

LBL-13379 c.2

DISCLAIMER

This document was prepared as an account of work sponsored by the United States Government. While this document is believed to contain correct information, neither the United States Government nor any agency thereof, nor the Regents of the University of California, nor any of their employees, makes any warranty, express or implied, or assumes any legal responsibility for the accuracy, completeness, or usefulness of any information, apparatus, product, or process disclosed, or represents that its use would not infringe privately owned rights. Reference herein to any specific commercial product, process, or service by its trade name, trademark, manufacturer, or otherwise, does not necessarily constitute or imply its endorsement, recommendation, or favoring by the United States Government or any agency thereof, or the Regents of the University of California. The views and opinions of authors expressed herein do not necessarily state or reflect those of the United States Government or any agency thereof or the Regents of the University of California.

LBL-13379

Do Nuclei Flow at High Energies?*

M. Gyulassy, K.A. Frankel, H. Stöcker

Nuclear Science Division
Lawrence Berkeley Laboratory
University of California
Berkeley, CA 94720

Nuclear flow patterns for E_{lab} = 250 MeV/nucleon are generated using the cascade code of Cugnon et al. and analyzed in terms of the kinetic flow tensor. The effect of increasing the nucleon-nucleon cross section and the difference between repulsive and stochastic scattering styles are studied. Flow patterns similar to hydrodynamic ones are found for $\sigma_{eff} \approx 3\ \sigma_{NN}$ and repulsive in-plane scattering style. A flow diagram is proposed to aid the experimental search for such flow patterns.

PACS 24.10-i,25.70.Fg,5.70.Ln

*This work was supported by the Director, Office of Energy Research, Division of Nuclear Physics of the Office of High Energy and Nuclear Physics of the U.S. Department of Energy under Contract W-7405-ENG-48 and by Deutscher Akademischer Austausch Dienst, Bonn, West Germany.

An important motivation for studying nuclear collisions at energies $\sim$1 GeV/nucleon is the hope the nuclear matter equation of state, $W(\rho,\tau)$, could be deduced experimentally. Currently, only the properties of W in the neighborhood of normal densities, $\rho \approx \rho_0 = 0.15\ \mathrm{fm}^{-3}$, and low temperatures, $\tau << E_F = 35$ MeV, are known. It would be desirable to constrain W at high densities and temperatures not only because it would test competing many body theories but also because such properties are essential for astrophysical problems such as supernova explosions and neutron stars. However, the program to extract $W(\rho,\tau)$ from nuclear collision data relies on the assumption that hydrodynamics provides an adequate dynamical framework at such energies. A necessary condition[1] for the validity of hydrodynamics is that the nucleon mean free path, $\lambda = (\sigma_{NN}\rho)^{-1}$, is much smaller than the dimension of the interaction region, $R \sim (\rho_0/\rho)A^{1/3}$ fm. Clearly, Ne + Ne and Ar + Ar collisions do not satisfy well the condition $\lambda << R$, and finite particle effects have been shown to be crucial[2] for such small systems. On the other hand, it is not <u>a priori</u> obvious that even Pb and U systems will exhibit hydrodynamic behavior, since λ/R is still only 1/4 for U.

Until recently, experimental tests of hydrodynamic behavior have focused on inclusive data. In particular, the data[3] on Ne (393 MeV/nucleon) + U $\rightarrow$ f + X with f = p,d,t have been compared with extensive hydrodynamic[1,4,5] and intranuclear cascade[6,7] calculations. The results indicate that such impact parameter averaged inclusive data are rather insensitive to dynamical details and are consistent with both fluid and cascade behavior to within numerical uncertainties.

New data[8] on central triggered Ne + U have provided, on the other hand, a more stringent test of dynamical models. The main new qualitative feature of those data is a suppression of the yield of p,d, and t fragments at low

energies ($E < 50$ MeV/nucleon) in the forward direction ($\theta_{lab} < 30°$). This is in contrast to the inclusive data[3] and to intranuclear cascade calculations,[6,7] which exhibit a maximum yield at $\theta_{lab} = 0°$. The agreement of recent hydrodynamic plus evaporation calculations with the qualitative features of those data provides at this time the strongest indication that hydrodynamic flow may occur in nuclear collisions.[9] However, because these calculations fail to reproduce the high energy ($E > 50$ MeV/nucleon) fragment spectra and because cascade calculations that include composite formation can also lead to suppression of light fragments in the forward direction,[10] no definitive conclusions can yet be drawn from the present data.

In order to test possible hydrodynamic behavior more directly, it has been proposed that exclusive variables such as the longitudinal energy fraction,[11] bounce angle,[12] thrust,[13] and sphericity[14] should be measured. With such exclusive variables it is easy to differentiate between gas and fluid behavior. The former[6] leads to collective flow only near the beam direction, while fluid dynamics[12] predicts significant collective flow at finite angles.

To understand better this qualitative difference between cascade and fluid results we investigate in this letter the transition from transparency to thermalization and finally to hydrodynamic flow as a function of particle number, A, and effective nucleon-nucleon cross section, σ_{eff}. By increasing A or σ_{eff}, we decrease λ/R and can hope to see the onset of hydrodynamic flow for sufficiently small λ/R. The cascade program developed by Cugnon et al.[6] is used to generate exclusive "data" as a function of A and σ_{eff}. We analyze the flow patterns by constructing the kinetic flow tensor event by event. This tensor is the natural generalization of sphericity[14,15] to reactions in which composite fragments are produced.

To associate a flow pattern or an event shape with a set of measured final momenta $\{\underset{\sim}{p}(\nu):\nu = 1,N\}$ the simplest procedure is to construct a weighted flow tensor:

$$F_{ij} = \sum_{\nu=1}^{N} w_\nu p_i(\nu)p_j(\nu) \quad , \tag{1}$$

where w_ν is the weight given to fragment ν. The familiar sphericity tensor[14,15] follows when w_ν is a constant, independent of ν. In terms of the eigenvalues f_n and orthonormal eigen (column) vectors e_n of F,

$$F = f_1 e_1 e_1^+ + f_2 e_2 e_2^+ + f_3 e_3 e_3^+ \quad , \tag{2}$$

In diagonal form F specifies an ellipsoid in momentum space with principal axes along e_n and radii $\sqrt{f_n}$. A cigar pattern, which is oriented along the z axis, would lead to $f_1 > f_2 = f_3$ and $e_1 = \hat{z}$, $e_2 = \hat{x}$, $e_3 = \hat{y}$. A pancake pattern would have $f_1 < f_2 = f_3$. Of course, many shapes such as an elbow cannot be adequately represented by F. However, we find that for flow patterns in nuclear collisions the ellipsoid specified by F provides a convenient characterization of event shapes. This is especially true for symmetric, A + A, collisions.

The eigenvalues satisfy the cubic equation

$$f_n^3 + a_2 f_n^2 + a_1 f_n + a_o = 0 \quad , \tag{3}$$

with

$$a_2 = -(F_{11} + F_{22} + F_{33}) \quad , \tag{4}$$

$$a_1 = F_{11}F_{22} + F_{11}F_{33} + F_{22}F_{33} - F_{12}^2 - F_{13}^2 - F_{23}^2 \quad , \tag{5}$$

$$a_o = F_{11}F_{23}^2 + F_{22}F_{13}^2 + F_{33}F_{12}^2 - F_{11}F_{22}F_{33} - 2F_{12}F_{13}F_{23} \quad , \tag{6}$$

The three real solutions (n = 1,2,3) can be compactly written as

$$f_n = -\frac{1}{3}a_2 + 2p\cos\left[\frac{1}{3}\cos^{-1}\left(\frac{r}{p^3}\right) + (n-1)\frac{2\pi}{3}\right] \tag{7}$$

in terms of the standard auxiliary variables

$$p = \frac{1}{3}(a_2^2 - 3a_1)^{1/2} \quad , \tag{8}$$

$$r = (a_1a_2 - 3a_o)/6 - a_2^3/27 \quad . \tag{9}$$

The eigenvectors are most conveniently evaluated in polar coordinates $[e_n^+ = (\sin\theta_n\cos\phi_n, \sin\theta_n\sin\phi_n, \cos\phi_n)]$ with polar and azimuthal angles given by

$$\cos\theta_n = \left\{1 + c_n^2 + (f_n - F_{33} - F_{23}c_n)^2/F_{13}^2\right\}^{-1/2} \quad ,$$

$$\tan\phi_n = c_nF_{13}/(f_n - F_{33} - F_{23}c_n) \quad , \tag{10}$$

with $\quad c_n = (e_n\cdot\hat{y})/(e_n\cdot\hat{z})$ given by

$$c_n = \frac{(F_{11}-f_n)\cdot(F_{33}-f_n) - F_{13}^2}{F_{12}F_{13}-F_{23}(F_{11}-f_n)} \quad . \tag{11}$$

The three orthogonal flow vectors that specify the event shape can now be defined in polar coordinates to be

$$\underset{\sim}{f}_n = (f_n, \theta_n, \phi_n) \quad . \tag{12}$$

Note that by symmetry (θ_n,ϕ_n) is equivalent to $(\pi-\theta_n,\phi_n+\pi)$ in specifying the event orientation.

Eqs. (3-12) apply of course with any weight w_ν in eq. (1). To choose an appropriate weight for nuclear flow patterns, we recall[13] that the most serious deficiency of sphericity (w_ν = constant) is that composite nuclear fragments are weighed incorrectly. For example, an α particle contributes

four times the amount to sphericity as four free nucleons with the same energy per nucleon. Thrust analysis, which is linear in particle momentum, was therefore proposed[13] to get around this problem. However, thrust is inconvenient since it is nonanalytic and requires a numerical sorting procedure.[15] To achieve the correct weighting of composites while retaining the simple analytic properties of sphericity, we propose to use $w_\nu = (2m_\nu)^{-1}$, where m_ν is the mass of the νth fragment. Therefore, we construct the kinetic flow tensor

$$F_{ij} = \sum_\nu p_i(\nu)p_j(\nu)/2m_\nu \ . \tag{13}$$

We emphasize that event shape analysis makes sense only in the nucleus-nucleus center of mass system since the eigenvalues of F specify an ellipsoid centered at the origin.

Note that the longitudinal energy fraction proposed in Ref. (11) is simply $F_{33}/\mathrm{Tr}F$. The kinetic flow tensor contains substantially more information (six independent numbers) than F_{33} and has a simpler, more intuitive interpretation than the Legendre coefficients of the angular pattern.[11] On the other hand, the Legendre coefficients of the event in the rotated coordinate system spanned by the e_n would be well suited to describe pear shape events for asymmetric reactions such as Ne + U.

Having determined six independent numbers $\{f_1, f_2, f_3, \theta_1, \phi_1, \theta_2\}$ from F, the question remains how to plot optimally the results. We propose the following flow diagram to characterize the range of three dimensional event shapes. First order the flow eigenvalues such that $f_1 > f_2 > f_3$ so that θ_1 is the polar angle of the maximum kinetic flow. We will call θ_1 the flow angle θ_F. The flow diagram is obtained by plotting θ_F versus the kinetic flow ratios f_1/f_3 and f_2/f_3 on the same plot. For

a fixed θ_F, a sphere corresponds to $f_1/f_3 = f_2/f_3 = 1$, while a cigar with major axis rotated by θ_F corresponds to $f_1/f_3 > f_2/f_3 = 1$. A squashed cigar has $f_1/f_3 > f_2/f_3 > 1$. A pancake event with a normal oriented along the beam axis corresponds to a flow angle $\theta_F = 90°$ and $f_1/f_3 = f_2/f_3 > 1$. An important experimental advantage of the flow diagram is that the ratios f_1/f_3, f_2/f_3 are insensitive to missed particle such as neutrons. In other words, the event shape is insensitive to random thinning of the momentum set $\{\underset{\sim}{p}(\nu)\}$.

In Fig. 1, we show the flow plot for Ne + Ne, Ar + Ar, and U + U at E_{lab} = 250 MeV/nucleon. This energy was chosen to maximize sensitivity to dynamical details.[16] Indicated along the boundaries are typical aspect ratios and orientations of the ellipses defined by a given θ_F and flow ratio. Recall that $\sqrt{f_1/f_3}$ and $\sqrt{f_2/f_3}$ are the aspect ratios in momentum space. For this plot the free space cross sections and standard stochastic NN scattering style (θ_{NN} chosen at random from $d\sigma_{NN}/d\Omega_{cm}$, ϕ_{NN}^{cm} chosen randomly between 0 and 2π at the distance of closest approach) were used in the cascade calculation. For Ne and Ar, 50 events were generated at each impact parameter, b/b_{max} = 0, 0.1, ..., 0.9. For U, 10 events per b were generated. It is important to emphasize that in contrast to differential cross section, event shapes can be determined from a relatively small number of events. The average values $\langle\theta_F\rangle_b$, $\langle f_1/f_3\rangle_b$, $\langle f_2/f_3\rangle_b$ as a function of impact parameter are indicated by points along the curves in units of $b_{max}/10$. Since the probability that the impact parameter lies between b and b + db is proportional to b, the numbers beside the symbols also indicate the relative intensity of such event shapes. Thus, standard cascade[6] predicts that there are five times more events with $\theta_F \approx 10°$ and $f_1/f_3 \approx 5$ than with $\theta_F \approx 25°$ and $f_1/f_3 \approx 2.5$ for Ne + Ne.

For all A, the largest θ_F occurs for b = 0. However, the flow characteristics are strongly A dependent. For b = 0, θ_F = 26 ± 20, 40 ± 25, 46 ± 28, 77 ± 9, and f_1/f_3 = 2.3 ± 0.6, 1.7 ± 0.3, 1.4 ± 0.1, 1.2 ± 0.1 for A = 20, 40, 100 (not plotted), 238 respectively. The ±Δ numbers indicate the rms fluctuations around the mean values due to finite particle number effects. The numerical uncertainties of the mean values is estimated to be $\Delta/\sqrt{n}$, where n is the number of events analyzed. In terms of a contour or scatter flow plot the average values define a ridge and Δ indicates the thickness of that ridge. The gap between $f_1/f_3 \approx 2.3$ and $f_2/f_3 \approx 1.5$ for b = 0 Ne + Ne as well as the large rms fluctuations indicate that Ne is too small to thermalize completely. Even though the Ar ridge and U ridge coincide for $b/b_{max} > 0.2$, note that the points are out of phase with $f_1/f_3(Ar) > f_1/f_3(U)$ for each fixed b. Thus, Ar is also much more transparent than U. It is nevertheless clear from Fig. 1 that there is a continuous evolution of event shapes as A increases to smaller aspect ratios and larger flow angles.

The most interesting question is whether U + U has reached the (nonviscous) hydrodynamic limit. The answer using standard cascade is no. We can determine one point on the flow diagram from existing hydrodynamic calculations. From Ref. 11, $F_{33}/TrF \approx 0.17$ for b = 0 corresponding to $\theta_F = 90°$, $f_1/f_3 = f_2/f_3 \approx 2.4$ as shown by the arrow in Fig. 1. This is a pancake shape of diameter ∿1.5 times its thickness. In contrast, the cascade produces near isotropy for U + U.

Therefore, we find a continuous transition from transparency to the isotropic thermalization as a function of A. However, standard intranuclear cascade[6] does not converge to the fluid limit. We have also done A + A calculations with A = 500, 1000, 2000, and have observed no more collective flow than with U.

Besides increasing A we have tried using larger effective NN cross sections to induce fluid behavior. In Fig. 2 the results for U + U using $\sigma_{eff} = 3\sigma_{NN}$ are shown by curves S3. Such large σ_{eff} could arise, for example, if critical scattering phenomena[17] would occur in nuclear collisions or if many body forces become important at high densities. Although the flow angle increases for fixed b relative to those in Fig. 1 with $\sigma_{eff} = \sigma_{NN}$, the flow at b = 0 is still far weaker than the hydrodynamic point. We conclude that $\lambda/R \ll 1$ is not sufficient for fluid behavior.

Could flow be sensitive to the details on the NN scattering style? Recall that the standard scattering style corresponds to a stochastic classical force with a <u>random</u> sign.[18] Therefore, the momentum transfer, $\underset{\sim}{q}$, and the relative coordinate, $\underset{\sim}{r}$, between two nucleons at the scattering time are assumed to be completely uncorrelated. Classically, on the other hand, any potential leads to definite correlations between $\underset{\sim}{q}$ and $\underset{\sim}{r}$. For example, a repulsive potential leads to

$$\underset{\sim}{q}\cdot\underset{\sim}{r} > 0 \text{ and } \underset{\sim}{q}\cdot(\underset{\sim}{r} \times \underset{\sim}{p}) = 0 \quad , \tag{14}$$

where $\underset{\sim}{p}$ is the incident relative momentum of the two nucleons. Equation (14) specifies the repulsive, in-scattering plane style as considered in Ref. (18). We have performed cascade calculations imposing eq. (14). With $\sigma_{eff} = \sigma_{NN}$ no significant difference was found in the flow diagram between stochastic and repulsive scattering styles. However, with $\sigma_{eff} = 3\sigma_{NN}$ we find (comparing curves S3 with P3 in Fig. 2) considerable dependence on style. Only the nonrandom style eq. (14) leads to collective flow similar to nonviscous hydrodynamic flow. As σ_{eff} increases the flow becomes more pronounced. For $\sigma_{eff} = 5\sigma_{NN}$ with eq. (14) style (curve P5), the flow ratio f_1/f_3 even exceeds the fluid value[11]. Thus, the flow obtained with nonviscous 1-fluid hydrodynamics represents only one possible class of flow patterns as a function of b. We conjecture that the variations of σ_{eff} and scattering

style considered here correspond in terms of viscous hydrodynamics to substantial variations in the transport properties of nuclei. For example, stochastic scattering (S3) may lead to larger viscosity effects than repulsive scattering (P3) thereby damping flow gradients. Also, P5 could lead to larger flow gradients than nonviscous hydrodynamics by simulating high immiscibility of projectile and target nuclei. These conjectures are currently under investigation.

In conclusion, we have constructed a microscopic model that exhibits a wide spectrum of possible flow patterns. With the flow diagram proposed here it should be easy to determine from exclusive data whether and how actual nuclei flow.

We are very grateful to J. Cugnon for making his cascade code available for our studies. This work was supported by the Director, Office of Energy Research, Division of Nuclear Physics of the Office of High Energy and Nuclear Physics of the U.S. Department of Energy under Contract W-7405-ENG-48 and by Deutscher Akademischer Austausch Dienst, Bonn, West Germany.

References

1. J.R. Nix, Prog. Part. Nucl. Phys. 2 (1979) 237;
   H. Stöcker et al., Prog. Part. Nucl. Phys. 4 (1980) 133.
2. J. Knoll, Phys. Rev. C20 (1979) 773; Nucl. Phys. A343 (1980) 511.
3. A. Sandoval, et al., Phys. Rev. C21 (1980) 1321.
4. J.R. Nix, D. Strottman, Phys. Rev. C23 (1981) 2548;
   A.A. Amsden, et al., Phys. Rev. C15 (1977) 2059.
5. H. Stöcker, et al., Z. Phys. A290 (1979) 297; A293 (1979) 173;
   A294 (1980) 1; Phys. Rev. Lett. 44 (1980) 725.
6. J. Cugnon et al., Nucl. Phys. A352 (1981) 505; Phys. Rev. C22 (1981) 2094.

7. Y. Yariv, Z. Fraenkel, Phys. Rev. C20 (1979) 2227; C24 (1981) 488: J.D. Stevenson, Phys. Rev. Lett. 41 (1978) 1702.

8. R. Stock et al., Phys. Rev. Lett. 44 (1980) 1243.

9. H. Stöcker, et al., LBL-12634, preprint (1981).

10. M. Gyulassy, R.A. Remler, K.A. Frankel, to be published.

11. G. Bertsch, A.A. Amsden, Phys. Rev. C18 (1978) 1293.

12. H. Stöcker, et al., LBL-11774 preprint (1980); G. Buchwald, et al., Phys. Rev. C24 (1981) 135.

13. J. Kapusta, Dan Strottman, LA-UR-81-795 preprint (1981); E. Farhi, Phys. Rev. Lett. 39 (1977) 1587.

14. J. Knoll, GSI-81-18 preprint (1981)

15. S. Brandt, H.D. Dahmen, Part. Fields C1 (1979) 61; S.L. Wu, G. Zobernig, Part. Fields C2 (1979) 107.

16. H. Stöcker, M. Gyulassy, J. Boguta, Phys. Lett. 103B (1981) 269.

17. M. Gyulassy, W. Greiner, Ann. Phys. 109 (1977) 485.

18. E. Halbert, Phys. Rev. C23 (1981) 295.

Figure Captions

1. Flow diagram showing the average polar angle of the maximum kinetic flow versus average flow ratios f_1/f_3 (solid) and f_2/f_3 (dashed). Symmetric A + A collisions "data" at 250 MeV/nucleon were computed via the cascade code of Cugnon et al.[6] The numbers beside the symbols refer to the value of b/b_{max} in steps of 0.1. The arrow locates the nonviscous hydrodynamic flow pattern[11] for b = 0.

2. As Fig. 1, for U + U at 250 MeV/nucleon as function of scattering style. S3 and P3 correspond to stochastic and eq. (14) scattering styles, respectively, with $\sigma_{eff}/\sigma_{NN} = 3$; P5 corresponds to eq. (14) with $\sigma_{eff}/\sigma_{NN} = 5$.

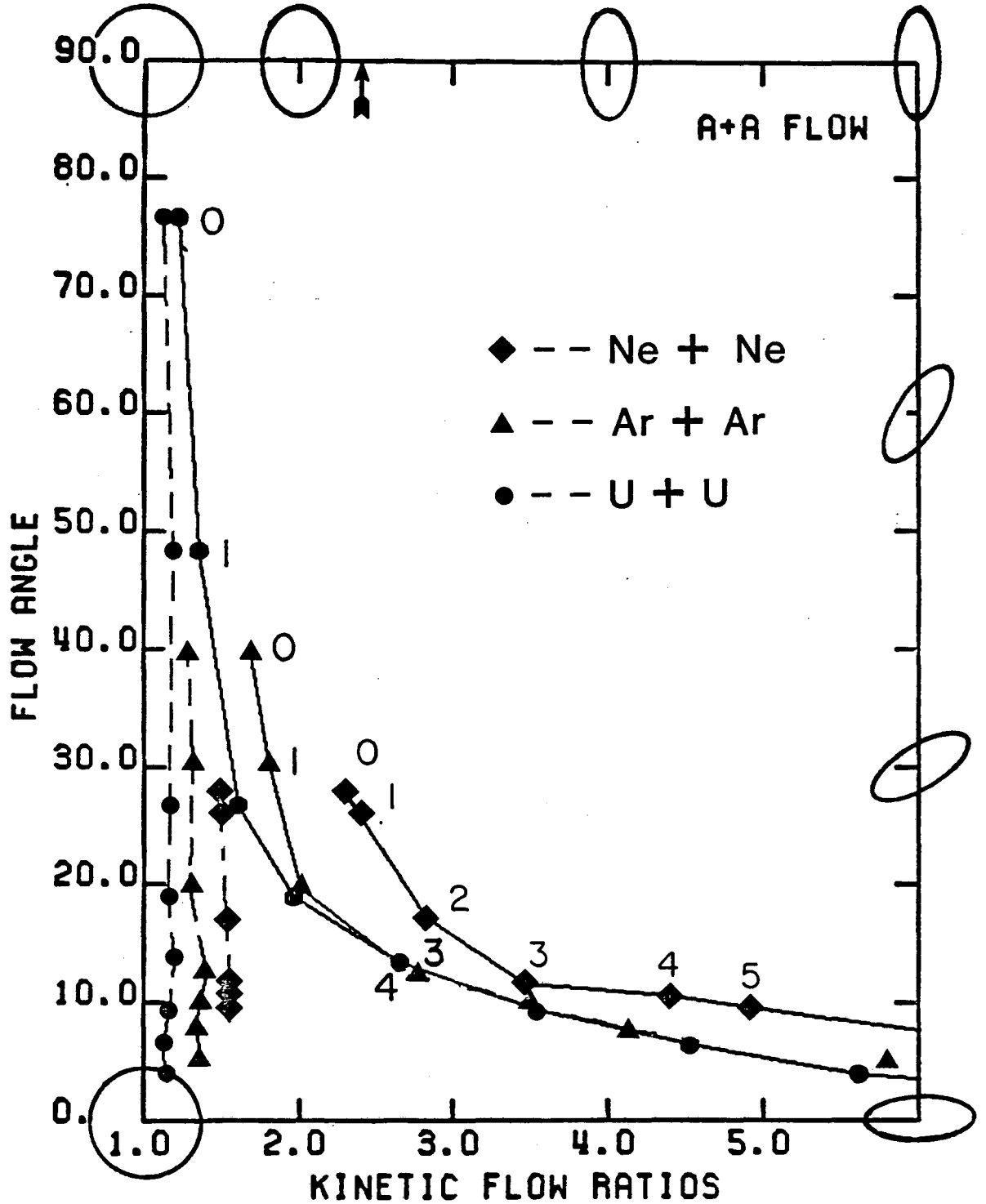

XBL 819-4955

Fig. 1

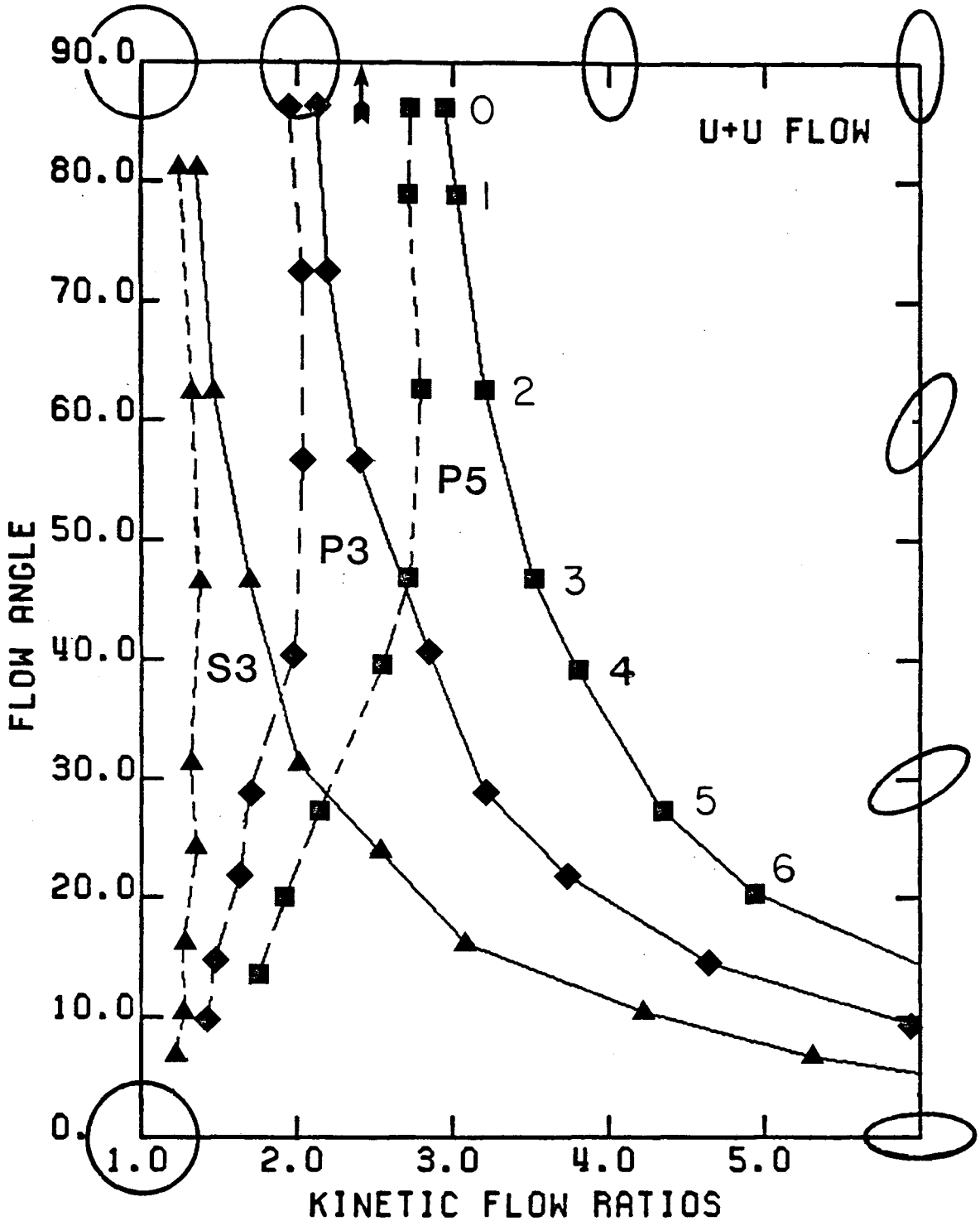

XBL 819-4954

Fig. 2

This report was done with support from the Department of Energy. Any conclusions or opinions expressed in this report represent solely those of the author(s) and not necessarily those of The Regents of the University of California, the Lawrence Berkeley Laboratory or the Department of Energy.

Reference to a company or product name does not imply approval or recommendation of the product by the University of California or the U.S. Department of Energy to the exclusion of others that may be suitable.

TECHNICAL INFORMATION DEPARTMENT
LAWRENCE BERKELEY LABORATORY
UNIVERSITY OF CALIFORNIA
BERKELEY, CALIFORNIA 94720